nature ecology & evolution

ARTICLES

PUBLISHED: 20 MARCH 2017 | VOLUME: 1 | ARTICLE NUMBER: 0094

Adaptation of phytoplankton to a decade of experimental warming linked to increased photosynthesis

C.-Elisa Schaum[1]*, Samuel Barton[1], Elvire Bestion[1], Angus Buckling[1], Bernardo Garcia-Carreras[2], Paula Lopez[1], Chris Lowe[3], Samraat Pawar[2], Nicholas Smirnoff[4], Mark Trimmer[5] and Gabriel Yvon-Durocher[1]*

Phytoplankton photosynthesis is a critical flux in the carbon cycle, accounting for approximately 40% of the carbon dioxide fixed globally on an annual basis and fuelling the productivity of aquatic food webs. However, rapid evolutionary responses of phytoplankton to warming remain largely unexplored, particularly outside the laboratory, where multiple selection pressures can modify adaptation to environmental change. Here, we use a decade-long experiment in outdoor mesocosms to investigate mechanisms of adaptation to warming (+4 °C above ambient temperature) in the green alga *Chlamydomonas reinhardtii*, in naturally assembled communities. Isolates from warmed mesocosms had higher optimal growth temperatures than their counterparts from ambient treatments. Consequently, warm-adapted isolates were stronger competitors at elevated temperature and experienced a decline in competitive fitness in ambient conditions, indicating adaptation to local thermal regimes. Higher competitive fitness in the warmed isolates was linked to greater photosynthetic capacity and reduced susceptibility to photoinhibition. These findings suggest that adaptive responses to warming in phytoplankton could help to mitigate projected declines in aquatic net primary production by increasing rates of cellular net photosynthesis.

The formation of organic carbon by phytoplankton (net primary production, NPP) is a key flux in the carbon cycle[1,2], contributing to nearly half of the carbon dioxide fixed globally on an annual basis[3,4]. There are currently major concerns that global warming will reduce aquatic NPP, due to increased nutrient limitation[5], and because rates of respiration and zooplankton grazing tend to be more sensitive to rising temperatures than those of photosynthesis[6–8]. These projections, however, do not account for the capacity for phytoplankton to adapt rapidly to environmental change. Although ample evidence for rapid evolutionary responses in phytoplankton to warming exists[9–11], our current understanding is based on highly simplified laboratory experiments, where populations are allowed to adapt free from natural enemies or competitors and where individual abiotic variables are manipulated in isolation. Consequently, we lack understanding of the mechanisms that govern evolutionary responses of phytoplankton to warming in sufficient detail and under a realistic ecological context, to capture the dynamics of thermal adaptation in models of aquatic biogeochemistry[5–8].

Phytoplankton growth depends on the balance between gross photosynthesis (P) and respiration (R)[12]. Crucially, as rates of R rise more rapidly with increases in temperature than do rates of P, the amount of carbon that can be allocated to growth after accounting for R declines rapidly as temperatures rise[10]. This imposes a physiological constraint on growth after acute exposure to high temperatures. Laboratory experiments have shown that phytoplankton can overcome this constraint and rapidly adapt to warming by down-regulating rates of R, thereby increasing the potential for carbon to be allocated to growth[10]. If general, this suggests that the mechanism underpinning evolutionary responses to warming in phytoplankton might also help to offset the short-term, exponential effects of temperature on rates of phytoplankton respiration and projected declines in aquatic primary production[6–8]. However, along with the vast majority of microbial evolution experiments, this mechanism was identified in isolated populations, evolving under controlled conditions in the laboratory. These experiments allow for highly controlled and replicated hypothesis testing, but their applicability in nature may be limited if interactions with other species and/or other components of the abiotic environment influence evolutionary responses to environmental change[13–15].

Here, we leverage a decade-long warming experiment in outdoor mesocosms[16] (Supplementary Fig. 1) to investigate the mechanisms of thermal adaptation in the green alga *Chlamydomonas reinhardtii*, embedded in complex, semi-natural ecosystems. Experimental warming has caused fundamental changes to the structure and biodiversity of the phytoplankton communities in these systems[17]; however, several highly abundant core taxa, including *C. reinhardtii*, are cosmopolitan across the warmed (+4 °C) and ambient mesocosms. This experimental system therefore provides an opportunity to quantify the mechanisms of adaptation to warming in the context of naturally assembled communities. In line with laboratory experiments on the green alga *Chlorella vulgaris*[10], we hypothesized that evolutionary changes in metabolic traits, which increase net photosynthesis and thereby the potential for carbon

[1]Environment and Sustainability Institute, University of Exeter, Penryn Campus, Penryn, Cornwall TR10 9EZ, UK. [2]Department of Life Sciences, Imperial College London, Silwood Park Campus, Ascot, Berkshire SL5 7PY, UK. [3]Biosciences, Daphne du Maurier Building, University of Exeter, Penryn Campus, Penryn, Cornwall TR10 9FE, UK. [4]School of Biological and Chemical Sciences, Queen Mary University of London, London E1 4NS, UK. [5]Geoffrey Pope Building, University of Exeter, Exeter EX4 4QD, UK. *e-mail: c.l.schaum@exeter.ac.uk; g.yvon-durocher@exeter.ac.uk

allocation to growth, will also play a role in adaptation to long-term warming in populations of *C. reinhardtii* embedded in complex semi-natural ecosystems.

Results

Patterns of local adaptation. We measured population growth rates across a gradient of eight temperatures (16–42 °C) to determine whether the traits that characterized the thermal dependence of growth differed between warmed and ambient isolates. T_h, which determines the upper temperature at which growth rates are 50% inactivated (see equation (5) in Methods), was the only parameter that differed significantly between warm and ambient isolates (Fig. 1a; Supplementary Tables 4 and 5). As the thermal optima, T_{opt}, depend on T_h (see equation (6) in Methods), maximum growth rate was achieved at higher temperatures for isolates from the warmed mesocosms (ambient: 27.5 ± 0.32 °C (mean ± standard error); warmed: 29.12 ± 0.55 °C; Fig. 1b). At 30 °C, *C. reinhardtii* from the warmed mesocosms divided 1.5-fold faster than their counterparts from the ambient mesocosms.

We further investigated patterns of local adaptation by quantifying the competitive fitness of the warmed isolates in all possible pairwise combinations of warmed versus ambient isolates at 16 and 34 °C. Warm-adapted isolates had higher competitive fitness at both 16 and 34 °C (Fig. 2; likelihood ratio test comparing models with and without 'assay temperature': Δd.f. = 1, $\chi^2 = 90.91$, $P < 0.0001$). Despite their higher fitness overall, we also found that competitive fitness of the warmed isolates increased significantly between 16 and 34 °C (post-hoc Tukey test: $z = 3.8$, $P < 0.001$) and, in consequence, the fitness of the ambient isolates declined between 16 and 34 °C. These findings suggest that a trade-off is likely to exist but that 16 °C was not cold enough to observe a complete reversal of competitive dominance between the warmed and ambient strains. Indeed, minimum temperatures in the ambient mesocosms reach lows of 4 °C in winter, while those in the warmed treatments rarely fall below 9 °C[17]. Other factors beyond temperature also differ between the treatments following a decade of experimental warming, for example, differences in the composition of competitors and/or consumers[17] and could drive a trade-off that limits invasion *in situ* that we would not observe in our simple temperature manipulation experiments.

Differences in photochemistry between warmed and ambient isolates. In phytoplankton, growth ultimately depends on the rate of net photosynthesis (NP), that is, the amount of carbon fixed by *P* remaining after losses attributable to *R*[18]. Therefore, we explored whether the higher competitive fitness of the warm-adapted isolates, particularly at higher temperatures, was related to higher rates of photosynthesis. We characterized key indicators of photosynthetic performance at the common growth temperature (18 °C). We observed marked differences in the response of NP to irradiance, measured by O_2 evolution (Fig. 3a). Warm-adapted isolates had substantially greater maximum rates of NP on a per cell basis and rates peaked at higher irradiances (Fig. 3a; Supplementary Tables 2 and 3). These divergences were also reflected in photochemical traits measured via fast repetition rate fluorometry (FRRF). The relative rate of photosynthesis (rP), which is an estimate of electron transport through photosystem II (PSII), differed between the warmed and ambient isolates in much the same way as NP, with maximum rates of rP significantly higher in the warm-adapted isolates (Fig. 3b; Supplementary Tables 2 and 3). The proportion of PSII reaction centres in a closed state (*C*) was substantially lower in warmed isolates, particularly at high irradiance (Fig. 3c). Together, the O_2 evolution and fluorometry data indicate a greater overall capacity for photosynthesis in the warmed isolates, which is further supported by higher cellular concentrations of chlorophyll *a* (chl *a*; non-sequential type III ANOVA: $F_{1,17} = 14.97$, $P = 0.001$; Fig. 3f).

The warmed and ambient isolates also diverged markedly in their susceptibility to photoinhibition. Rates of NP via O_2 evolution saturated at 414 µmol quanta m^{-2} s^{-1} in the ambient isolates, after which they became strongly photoinhibited, declining to zero at around

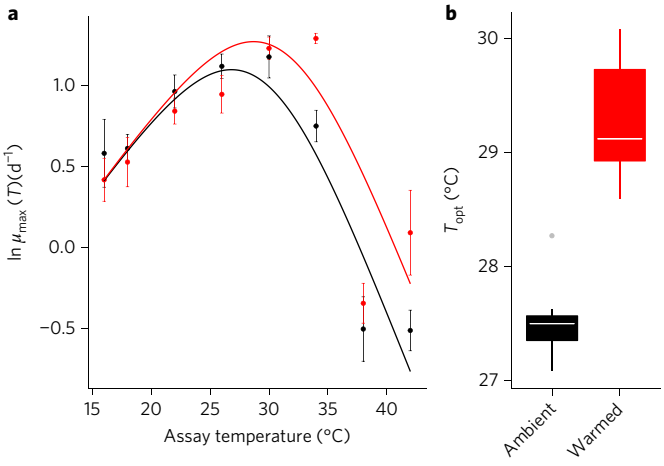

Figure 1 | Patterns of local thermal adaptation. a, Thermal reaction norms for growth rate across temperatures ranging from 16 to 42 °C demonstrate isolates of *C. reinhardtii* from the warmed mesocosms had higher optimal temperatures than their ambient counterparts. **b**, Box and whisker plot of the replicate-level optimum temperatures show median values for T_{opt} were higher in warmed (29.12 ± 0.55 °C) than the ambient (27.5 ± 0.32 °C) isolates. Fitted lines in **a** are derived from the fixed effects of the mixed effects model fitting the Sharpe–Schoolfied equation, equation (5), to the rate data. Data in **a** are plotted as treatment means with error bars ±1 s.e.m. Replicate level parameter estimates for T_{opt} in **b** are derived from the fixed and random effects of the mixed effects model. Tops and bottoms of boxes in box and whisker plots correspond, respectively, to the 25th and 75th percentiles, horizontal white lines correspond to medians, and whisker extents correspond to 1.5 × the interquartile range. Black denotes ambient treatments, red indicates warmed treatments.

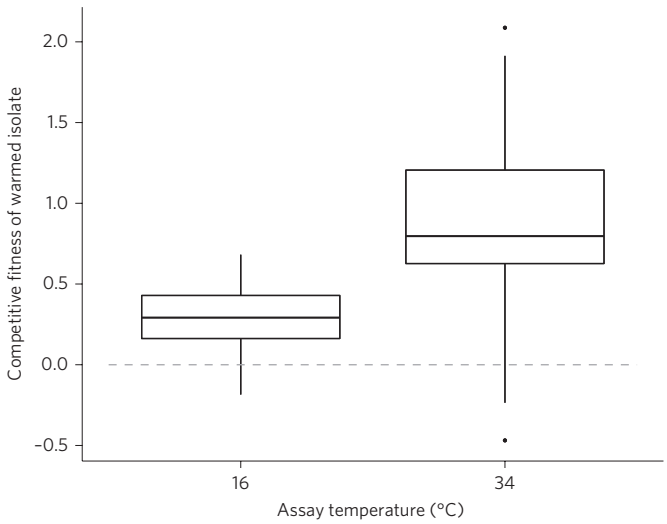

Figure 2 | Competitive fitness of the warmed relative to the ambient isolates at 16 and 34 °C. Competition coefficients of heated relative to ambient isolates were greater than 0 (dashed line) at both 16 and 34 °C, indicating that warmed isolates tended to outcompete ambient isolates in both environments. Competitive fitness of the warmed isolates was higher at 34 °C than at 16 °C. Tops and bottoms of boxes correspond, respectively, to the 25th and 75th percentiles, horizontal lines correspond to medians, and whisker extents correspond to 1.5 × the interquartile range.

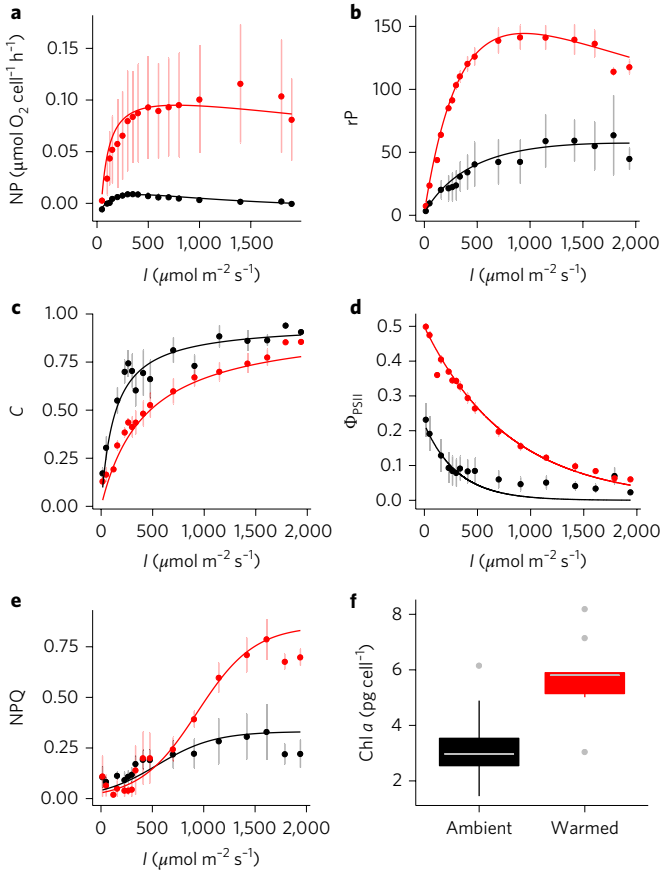

Figure 3 | Differences in photochemical traits between the warmed and ambient isolates. a, Photosynthesis–irradiance curves via O_2 evolution show higher maximum rates of NP and saturating irradiance in the warmed isolates. **b**, Rates of electron transport through PSII (rP) quantified by FRRF also differ between warmed and ambient isolates with higher maximum rates in the warmed isolates. However, note that rP in the ambient isolates continues to increase at irradiances above 500 μmol m^{-2} s^{-1} while O_2 evolution declines, suggesting O_2 photoreduction. **c**, The proportion of PSII reaction centres in a closed state, *C*, is lower in the warmed isolates, indicating greater photosynthetic capacity. **d**, The photochemical efficiency of PSII (Φ_{PSII}) was consistently higher and declined less steeply with increasing irradiance in the warmed isolates, highlighting a reduced susceptibility to photoinhibition. **e**, NPQ at high irradiance is substantially higher in the warmed isolates. **f**, Cellular concentrations of chl *a* were also higher in the warmed isolates, in line with their greater photosynthetic capacity and efficiency. Data are plotted as treatment means with error bars ±1 s.e.m. Fitted lines are derived from the fixed effects of the mixed effects models. Black denotes ambient treatments, red indicates warmed treatments.

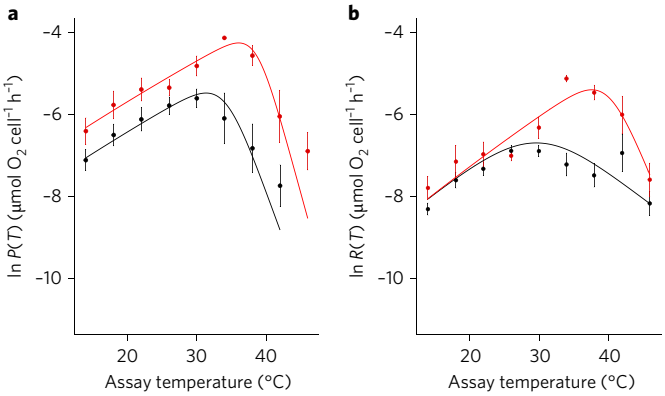

Figure 4 | Shifts in metabolic traits between warmed and ambient isolates. a, The acute thermal responses of per capita *P* show that warmed isolates have substantially higher specific rates of gross photosynthesis, $P(T_c)$, and optimal temperatures, T_{opt} than their ambient counterparts. **b**, Acute thermal responses for *R* demonstrate higher values for T_{opt} and the inactivation energy, E_h, in the warmed isolates. These data provide suggest evolved differences in the metabolism of isolates of *C. reinhardtii* from the warmed and ambient mesocosms. Data are plotted as treatment means with error bars ±1 s.e.m. Fitted lines are derived from the fixed effects of the mixed effects models fitting the Sharpe–Schoolfield equation, equation (5), to the rate data. Black denotes ambient treatments, while red indicates warmed treatments.

1,000 μmol quanta m^{-2} s^{-1} (Fig. 3a). The warmed isolates exhibited no such photoinhibition of NP (Fig. 3a). In support of these findings, the maximum quantum efficiency of PSII (F_v/F_m) was higher in the warmed isolates (Kruskal–Wallis test: $\chi^2_1 = 9.1$, $P = 0.003$) and photosynthetic efficiency (Φ_{PSII}; proportion of the total light absorbed by PSII that is used in photochemistry) in the warmed isolates exhibited a less pronounced decline with increasing irradiance than in their ambient counterparts (Fig. 3d). Notably in the ambient isolates, saturating irradiance was much higher for rP (optimal light intensity, I_{opt} = 1,835 μmol quanta m^{-2} s^{-1}) than NP via O_2 evolution (I_{opt} = 414 μmol quanta m^{-2} s^{-1}), while optimal light intensities for rP (I_{opt} = 953 μmol quanta m^{-2} s^{-1}) and NP (I_{opt} = 781 μmol quanta m^{-2} s^{-1}) in the warmed isolates were comparable (Fig. 3a,b). These data show that light-dependent electron transport in the ambient isolates continues at high irradiance while O_2 evolution is close to zero. A possible explanation for this difference is that a large proportion of the electron flux is driving O_2 photoreduction via the Mehler reaction[19] or the plastid terminal oxidase[20], resulting in a potentially photoprotective water–water cycle[21]. Clearly, however, O_2 photoreduction in the ambient isolates was still insufficient to prevent chronic photoinhibition. The warmed isolates most probably maintained a sufficiently high CO_2 assimilation capacity to allow a high electron transport rate to support development of greater levels of non-photochemical quenching, NPQ (Fig. 3e; Supplementary Tables 2 and 3). These results highlight that adaptation to warming conferred an apparent decrease in susceptibility to photoinhibition. While identification of the precise mechanism of the difference in photosynthetic characteristics of the ambient and warmed isolates requires further investigation, our data suggest that the evolution of increased tolerance to high temperatures (and therefore greater kinetic energy) is also associated with higher photosynthetic capacity and increased tolerance to high irradiance.

Adaptation to warming is linked to increased photosynthesis. To investigate further how differences in metabolism contribute to the increased fitness of the warm-adapted isolates, particularly at high temperatures, we quantified the responses of *P* and *R* to acute variation in temperature. As expected from the photosynthesis–irradiance curves, isolates from the warmed mesocosms had significantly higher rates of temperature-normalized gross photosynthesis ($P(T_c)$), inactivation energies (E_h) and T_h (Fig. 4; Supplementary Tables 4 and 5). Hence, rates of photosynthesis were generally greater and peaked at higher temperatures in the warm-adapted isolates (T_{opt} ambient: 31.4 ± 0. 60 °C, T_{opt} warmed: 36.0 ± 0.75 °C). For respiration, E_h and T_h were significantly higher in the isolates from the warmed mesocosms (Supplementary Table 4 and 5), meaning that rates of respiration also peaked at higher temperatures (ambient: 29.7 ± 0.91 °C, warmed: 37.6 ± 0.58 °C). Together, these analyses demonstrate substantial shifts in the traits that characterize the thermal responses of photosynthesis and respiration. A key question,

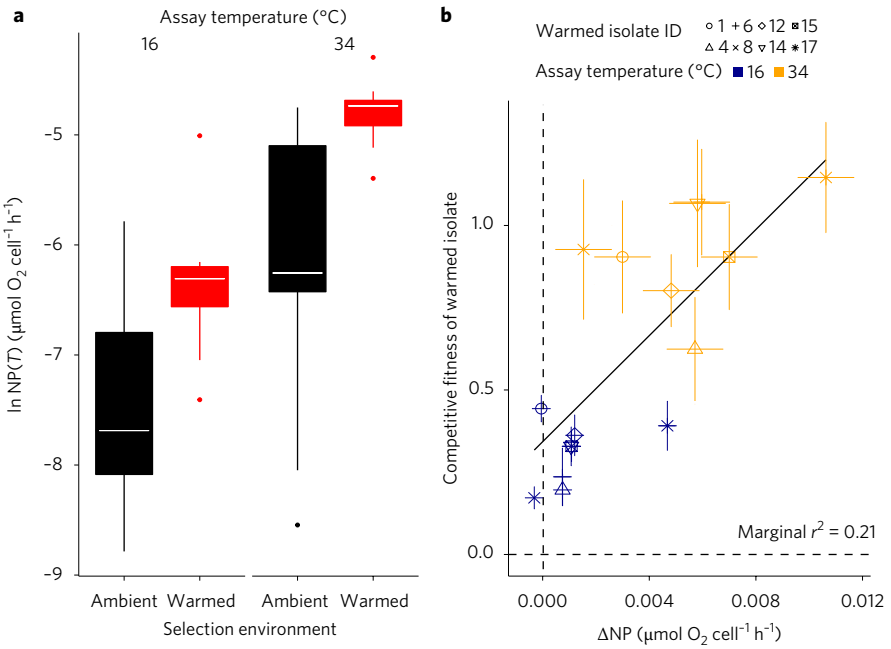

Figure 5 | Higher rates of NP are linked to greater competitive fitness in the warm-adapted isolates. a, Rates of NP were 3.5-fold higher in the warmed than the ambient isolates. Tops and bottoms of boxes in box and whisker plots correspond, respectively, to the 25th and 75th percentiles, horizontal white lines correspond to medians, and whisker extents correspond to 1.5 × the interquartile range. Black denotes ambient treatments, red indicates warmed treatments. **b**, Pairwise differences between warmed versus ambient isolates in rates of NP at 16 and 34 °C, ΔNP, are positively correlated with competitive fitness of the warmed isolates, such that higher rates of NP yield greater competitive fitness, which is nearly always the case in the warmed isolates. The fitted line is derived from the fixed effects of a linear mixed effects model and marginal r^2 estimates the variance explained by the fixed effects. Values above the dashed horizontal line indicate that warmed isolates outcompete their ambient counterparts. Values to the right of the dashed vertical line indicate that the rate of NP in the warmed isolate is greater than that of the ambient. Blue symbols denote competition assays carried out at 16 °C and orange symbols give assays carried out at 34 °C. *x* and *y* error bars represent ±1 s.e.m. on ΔNP and competitive fitness of the warmed isolates, respectively.

therefore, is whether evolutionary shifts in these metabolic traits contribute to enhancing the fitness of the warm-adapted isolates.

The average activation energy, E_a, which characterizes how metabolic rates increase below T_{opt}, was higher for *R* than *P* in both warmed and ambient isolates (Suppplementary Table 5), in line with previous work on green algae and vascular plants[6,10,22]. Consequently, *R* increased proportionately more with rising temperature than did *P*, meaning that the amount of *P* available for allocation to growth declined with acute increases in temperature. Warm-adapted isolates overcame this physiological constraint and were therefore fitter than the ambient isolates, particularly at higher temperatures, by up-regulating rates of $P(T_c)$, which served to increase the amount of photosynthetic carbon that could be allocated to growth. Note that the higher rates of photosynthesis in the warm-adapted isolates cannot be attributed to changes in cell size. We found no evidence for differences between warmed and ambient isolates in either the magnitude of plasticity in cell size (indexed by the gradient of the reaction norm for cell size with temperature) or average cell size at a given assay temperature (Supplementary Fig. 4).

If increases in $P(T_c)$ and optimal temperatures for *P* translate into higher rates of NP, then these shifts in metabolic traits could provide a mechanistic basis for the observed patterns of local thermal adaptation in community-embedded populations of *C. reinhardtii.* Consistent with this reasoning, we found evidence for significant main effects of 'assay temperature' and 'selection environment' on rates of cellular NP (Fig. 5a; likelihood ratio test comparing models with and without 'assay temperature': Δd.f. = 1, $\chi^2 = 57.89$, $P < 0.0001$; or 'selection environment': Δd.f. = 1, $\chi^2 = 21.38$, $P < 0.001$; to a full model with both main effects). Consequently, warm-adapted isolates had rates of NP that were 3.5-fold higher on average, compared with those from ambient mesocosms. On an isolate-by-isolate basis, we also saw that pairwise differences in NP between all combinations of warmed versus ambient isolates were positively correlated with the competitive fitness of the warmed isolates, indicating that isolates with high photosynthetic rates tended to outcompete those with low rates of NP (Fig. 5b; likelihood ratio test comparing models with and without 'ΔNP' as a covariate: Δd.f. = 1, $\chi^2 = 12.46$, $P < 0.05$). Furthermore, the magnitude of the pairwise fitness and photosynthetic differentials were largest at 34 °C (likelihood ratio test comparing models with and without 'assay temperature' as a factor: Δd.f. = 2, $\chi^2 = 62.22$, $P < 0.001$), where the warm-adapted isolates had substantially higher rates of NP and competitive fitness (Fig. 5b). Notably, however, higher photosynthetic rates were clearly not the only mechanism at play, because one of the isolates (pond 8) outcompeted its ambient counterparts at 16 °C, despite having lower average rates of NP (Fig. 5b). Thermal adaptation may have also altered cellular nitrogen and phosphorus quotas[23,24] in the warmed and ambient isolates, which could in turn impact on nutrient limitation, exudation of excess photosynthate and the coupling between growth, fitness and NP[25]. Indeed, a detailed understanding of the potential interactions between warming, nutrient limitation and adaptation could help account for some of the unexplained variation in the coupling between competitive fitness and net photosynthesis, and merits further investigation in future work. Nevertheless, the positive correlation between differentials of cellular net photosynthesis and competitive fitness on an isolate-by-isolate basis suggest that increases in photosynthetic capacity played an important role in the adaptation of *C. reinhardtii* to warming under ecologically realistic, semi-natural conditions.

Discussion

Understanding the capacity, variability and mechanisms that shape evolutionary responses of phytoplankton to warming is central to

predicting how rates of primary production and carbon sequestration will shift in the coming decades. Several recent studies have shown that adaptive responses of phytoplankton to warming are possible within time frames of months to years[9,10]. However, experiments investigating evolutionary responses to environmental change in algae have thus far dealt with greatly simplified conditions, maintaining an enemy- and competition-free space, and changing individual environmental variables in isolation. Our work builds on this knowledge by quantifying adaptive responses in *C. reinhardtii* in a semi-natural field setting to a decade of experimental warming. The outdoor mesocosms were originally seeded with a diverse assemblage of taxa, each of which consisted of heterogeneous populations probably comprising many genotypes. The mesocosms are also open to natural dispersal among the ponds and from the regional species pool. Consequently, local adaptation of *C. reinhardtii* to warming occurred in the context of heterogeneous founder populations and metapopulation dynamics (for example, dispersal, colonizations and local extinctions). As will be true of natural populations adapting to environmental change, the evolutionary divergence we observed will have occurred through a combination of selection acting on existing standing genetic variation within the founder- and meta-population, as well as *de novo* mutations. Our findings demonstrate that increased rates of cellular net photosynthesis played an important role in the adaptive response of *C. reinhardtii* to warming. This result is in qualitative agreement with a recent laboratory selection experiment on the green alga *C. vulgaris*, which showed that adaptation to elevated temperature was related to increases in the efficiency of photosynthetic carbon allocation to growth[10]. However, in *C. vulgaris*, increases in carbon availability were mediated by a decline in rates of respiration[10] as opposed to increases in photosynthetic rates observed here. Although the two experiments are in broad agreement, in that evolutionary shifts in metabolic traits mediate adaptive responses to warming, direct quantitative comparison should be interpreted cautiously, given the substantial differences in the temporal (months versus years), spatial (isolated flask versus open outdoor system) and organizational (population versus ecosystem) scales between the two studies. Nevertheless, if increases in photosynthetic carbon fixation are a general feature of adaptive responses of phytoplankton to warming, they could, at least partially, offset predicted declines in the carbon sequestration of aquatic ecosystems[2,5,7,16,17] owing to the exponential effects of temperature on respiratory CO_2 production.

Methods

The mesocosm experiment. Twenty freshwater mesocosms, each holding 1 m^3, were set up in 2005 to mimic shallow lake ecosystems[26]. They are situated at the Freshwater Biological Association's river laboratory (2° 10′ W, 50° 13′ N) in East Stoke, Dorset, UK (see Supplementary Fig. 1). Ten replicate mesocosms have been warmed to 4 °C above ambient temperature in accordance with the Intergovernmental Panel on Climate Change A1B global warming projections[27]. Warming is achieved by an electronic heating element connected to a thermocouple, which monitors the temperature in a given heated and unheated treatment pair. The mesocosms were seeded in December 2005 with organic substrates and a suite of organisms from surrounding natural freshwater habitats, and were then left open to natural colonization and dispersal mediated community assembly. We have previously shown that the warmed mesocosms have higher algal species richness, greater biomass and faster rates of *in situ* photosynthesis[17]. Crucially, however, temperature is the principal abiotic factor in the experiment; other variables (such as nutrient availability, light, day length) that are typically confounded with temperature along natural geographic or altitudinal gradients are consistent between the warmed and ambient treatments. This study system therefore provides a powerful tool to investigate evolutionary responses to climate change, because it enables characterization of adaptation to warming under complex semi-natural conditions, yet retains some of the control and replication afforded by an experimental approach.

Lineage isolation and culture. We isolated *Chlamydomonas*, a known cosmopolitan and highly abundant genus in the heated and ambient mesocosms[17], by first passing water through a 45 µm and then a 20 µm filter, followed by serial dilution and streaking the isolate on to agar-filled pipette tips turned towards a light source (enabling identification and isolation of motile autotrophs). Organisms putatively identified as *Chlamydomonas* were then grown on agar plates infused with Bold's basal medium (BBM). Colonies were then picked under a microscope, transferred back into liquid culture (autoclaved, filtered water taken from rainwater holding tanks at the mesocosm experiment supplemented with BBM at 1/3 the standard concentration) and kept at 18 °C (the average daytime temperature across treatments at the time of sampling) in a common garden for two weeks in semi-continuous batch culture (see also Supplementary Fig. 2). Taxonomy of *Chlamydomonas* was confirmed by microscopy and using PCR followed by Sanger sequencing within the 18S sequence using a set of primers with forward sequence GAAGTCGTAACAAGGTTTCC and reverse sequence TCCTGGTTAGTTTCTTTTCC. Positive controls were run using p23 primers amplifying in the RuBisCO region, with forward GGACAGAAAGACCCTATGAA and reverse TYAGCCTGTTATCCCTAGAG. This yielded 18 of the 20 isolates with an at least 99% Basic Local Alignment Search Tool (BLAST) match for *C. reinhardtii,* 8 from heated and 10 from ambient mesocosms (see Supplementary Table 1). These were used throughout the experiments and the other 2 samples were discarded. BLAST matches based on 18S region results cannot always guarantee correct identification to the species level. However, *C. reinhardtii* was known to be present in the mesocosms based on surveys in 2007 and 2012[16,17], and is further discernable under the microscope from another cosmopolitan *Chlamydomonas* species in the mesocosm system, *C. globosa*[28]. We constructed a phylogenetic tree displaying the sequences from the isolates used in the experiments, alongside the *C. reinhardtii* BLAST hits that had the highest percentage identity to our samples and several other common chlorophytes: *C. globosa*, *Lobochlamys* and *C. vulgaris*. The tree was built on 'clustalw' alignment data in the 'phangorn' package in R and subsequently imported into FigTree[29]. The figure shows that isolates from the mesocosm experiment cluster with one another and with known Chlamydomonadaceae, but are on a separate branch to *C. vulgaris*.

Thermal response of growth and cell size. To determine how population growth, a proxy for fitness, and cell size, a trait that we expect to be highly phenotypically plastic, depended on temperature, isolates were grown at eight temperatures (16, 18, 22, 26, 30, 34, 38 and 42 °C) in parallel. The isolates were inoculated into mesocosm water amended with BBM to a starting density of 100 cells ml^{-1}, and cell densities and size were tracked daily on a flow cytometer (BD Accuri C6). Populations were transferred to fresh media once at each temperature during the middle of the logarithmic phase of growth, before being left to reach stationary phase. Abundance data were then fitted to a modified Gompertz model[30] using non-linear regression to estimate population growth rates at each assay temperature.

Non-linear curve fitting of Gompertz growth model was carried out using the 'nlsLM' function in the R package, 'minpack.lm'[31], which uses the Levenberg–Marquardt optimization algorithm. Parameter estimation was achieved by running 1,000 different random combinations of starting parameters picked from a uniform distribution and retaining the parameter set that returned the lowest Akaike information criterion (AIC) score.

We took two approaches to calibrating cell size from the forward scatter values returned by the flow cytometer. In the first, mixed communities taken from the mesocosms were passed through filters of different sizes (1, 2, 4, 5, 10, 20 and 40 µm) to create a known upper threshold for size. These filtered samples were then run on the flow cytometer along with calibration beads of known size (3–5 µm) and cross-checked under the microscope using the ImageJ software. In the second, we ordered axenic species of known size from a culture collection (see Supplementary Fig. 5 for details) and measured their average cell size (at least 100 images per species) using ImageJ software, while simultaneously running them on the flow cytometer. The data were then pooled to create calibration curves that allow for calculating cell size from the forward scatter (see Supplementary Fig. 5). Note that the calculated cell diameters are still approximate values and should be treated as such, but relative changes in cell size (for example, across different assay temperatures and treatments) remain valid and informative.

Photochemical traits. Photosynthesis measurements were made on all isolates when in the middle of the logarithmic phase of population growth. Aliquots (50 ml) of the populations were concentrated through centrifugation to a density of approximately 10^5 cells ml^{-1} and acclimatized to the assay temperature for 15 min in the dark before measuring metabolic rates. Photosynthesis–irradiance curves were quantified from 0 to 2,000 µmol m^{-2} s^{-1} at the common garden temperature (18 °C) using two approaches. First, NP was measured as O_2 evolution in a Clark-type oxygen electrode (Hansatech Ltd, King's Lynn, UK, Chlorolab2) at increasing light intensities in intervals of 50 µmol^{-1} m^{-2} s^{-1} up to 300 µmol^{-1} m^{-2} s^{-1}, and then in intervals of 100 µmol^{-1} m^{-2} s^{-1} up to 1,000 µmol^{-1} m^{-2} s^{-1}, followed by 200 µmol steps up to 2,000 µmol^{-1} m^{-2} s^{-1}. Rates of R were measured as O_2 consumption in the dark and P was estimated as $P = NP + R$. Rates were expressed on a per cell basis by normalizing by cell counts from each aliquot. Alongside the cell counts for phytoplankton, samples were also stained for bacterial load at the end of each run. Densities of bacteria were low (ca. 100 cells ml^{-1}), did not differ between warmed and ambient isolates and, given their comparatively small cell size, accounted for a tiny fraction of algal biomass. Thus, as confirmed from pilot experiments, filtering the cultures at 1 µm and running the filtrate through the O_2 electrode, bacterial

biomass density was insufficient to yield detectable O_2 uptake. Photosynthesis–irradiance curves for NP were fitted to a dynamic model of photoinhibition[32,33]:

$$P(I) = \frac{P_{max} I}{\frac{P_{max}}{\alpha I_{opt}^2} I^2 + \left(1 - 2\frac{P_{max}}{\alpha I_{opt}}\right) I + \frac{P_{max}}{\alpha}} - R \quad (1)$$

where $P(I)$ is the rate of photosynthesis at light intensity I, P_{max} is the maximum rate of photosynthesis at I_{opt}, α controls the rate at which $P(I)$ increases up to P_{max} and R is the rate of respiration (that is, the rate of O_2 flux when $I = 0$). We fitted the rate data to equation (1) using a non-linear mixed effects model via the 'nlme' package in R. The mixed effects model allowed us to account for the unbalanced design of our experiment (for example, eight warmed replicate isolates and ten ambient isolates) as well as its hierarchical nature (for example, replicate-level responses nested within the overall response across all replicates). Model fitting entailed starting with the most complex possible model, which included random effects by replicate on each of the parameters of equation (1) and 'selection environment' as a fixed two-level factor (for example, a 'heated' or an 'ambient' isolate) on each parameter. Random effects were removed when the estimated variances were very low, indicating an over-parameterized model. The significance of differences between 'warmed and 'ambient' isolates in each of the model parameters were determined through likelihood ratio tests on nested models with and without the 'selection environment' treatment. Model simplification stopped when all coefficients were significant ($P < 0.05$). The final models were then refitted with restricted maximum likelihood for parameter estimation.

We also characterized a range of photochemical parameters using FRRF (FastPro8, FRRf3, Fast Ocean System Chelsea Technology Group)[34]. This entailed adding 100 µl of dilute sample (cell count less than 1,000 cells ml^{-1}) to 5 ml of fresh culture medium. Samples were then pre-incubated in the dark at 18 °C (temperature of the common garden) for 15 min in a water bath, and another 10 min in the FRRF to make sure that they were fully dark acclimated and all reaction centres closed. Photochemical traits (see below for details) were measured in response to rapid flashes at increasing light intensities from 0 to1,900 µmol m^{-2} s^{-1}. Flash frequency and rate followed standard protocols for green algae[34], with 100 flashes of 1.1 µs at 1 µs intervals. Peak emission wavelengths of the LEDs used for excitations were at 450, 530 and 624 nm. Of the parameters returned by the FRRF, rP, NPQ, C and Φ_{PSII} were particularly relevant to our study, as they describe the light responses of photosynthetic efficiency and susceptibility to photoinhibition. rP data indicate the relative rate of photosynthesis in response to irradiance and are obtained as an estimate of electron transport through PSII. NPQ is a measure of the cell's ability to maintain photochemical function at high light intensities. C describes the proportion of PSII reaction centres in a closed state. Φ_{PSII} values are an indication of the proportion of the total light absorbed that is used in photochemical reactions in PSII.

To investigate the light response of the above parameters statistically, rP data were fitted to equation (1) as described above for O_2 evolution data. NPQ data were fitted to a logistic model (using 'SSlogis' in the 'nlme' package in R) with:

$$NPQ(I) = \frac{NPQ_{Asym}}{1 + e^{(I_{mid} - I)} / I_{scal}} \quad (2)$$

where NPQ_{Asym} describes the asymptote of the logistic function, I_{mid} the inflection point of the curve, where $NPQ(I_{mid})$ is $NPQ_{Asym}/2$. I_{scal} is a numeric scaling factor for I, the irradiance. C was fitted to a Michaelis–Menten function:

$$C(I) = C_{max} \frac{I}{K_s + I} \quad (3)$$

where C_{max} is the maximum value of C and K_s is the half-saturation constant, which gives I where C is half of its maximum value. We fitted Φ_{PSII} data to an exponential decay function:

$$\Phi_{PSII} = ae^{(bI)} \quad (4)$$

where a is a normalization constant and b is the rate constant that characterizes how rapidly Φ_{PSII} declines with increasing I. Equations (1) to (4) were fitted to the FRRF data with non-linear mixed effects models that included random effects by replicate on each parameter and 'selection environment' as a fixed two-level factor (for example, a 'warmed' or an 'ambient' isolate) on each parameter. Model selection proceeded in the same manner as described above for O_2 evolution data. Details on model selection and analysis of the results can be found in Supplementary Tables 2 and 3 (nomenclature and acronyms as given here). Dark adapted F_v/F_m, which gives the maximum potential efficiency of PSII, was analysed using a Kruskal–Wallis test on ranked data to account for unequal variance between treatments. F_v is the difference between maximum fluorescence and minimum fluorescence, that is, it is a measure of the dark-adapted fluorescence. F_m is the maximum fluorescence. F_v/F_m is a normalized ratio created by dividing variable fluorescence by maximum fluorescence.

Chl *a* content of the samples was measured using average per cell FL3 fluorescence as returned by an Accuri C6 flow cytometer. Calibration curves were established by regressing the average per cell FL3 fluorescence against chl *a* content (pg chl *a* $cell^{-1}$), measured on a spectrophotometer after pigment extraction in acetone. As with the size calibration data, although the absolute values of chl *a* are approximate, they nevertheless facilitate comparisons between treatments. We tested for differences between warmed and ambient isolates using a one-way ANOVA because the variance between treatments was approximately equal. To account for the unbalanced design, the ANOVA was carried out as a non-sequential type III ANOVA on unweighted means using the 'Anova' function in the 'car' package in R.

Quantifying thermal responses of growth and metabolism. Thermal tolerance curves for P at I_{opt} and R in the dark were quantified from 14 to 46 °C. Population growth (μ_{max}, Gompertz growth model) and per capita metabolic rates (that is, P and R) followed a unimodal response to temperature that could be quantified using the four-parameter Sharpe–Schoolfield model, which assumes that there is a single rate-limiting enzymatic reaction that is reversibly inhibited by temperature:

$$\ln(b(T)) = E_a\left(\frac{1}{kT_c} - \frac{1}{kT}\right) + \ln(b(T_c)) - \ln\left(1 + e^{E_h\left(\frac{1}{kT_h} - \frac{1}{kT}\right)}\right) \quad (5)$$

where $b(T)$ is the per capita metabolic rate (µmol O_2 $cell^{-1}$ h^{-1}), k is Boltzmann's constant (8.62×10^{-5} eV K^{-1}), E_a is an activation energy (in eV) for the metabolic process, T is temperature in Kelvin (K), E_h characterizes temperature-induced inactivation of enzyme kinetics above T_h, where half the enzymes are rendered non-functional and $b(T_c)$ is the rate of metabolism normalized to an arbitrary reference temperature, $T_c = 18$ °C, where no low or high temperature inactivation is experienced. Equation (5) yields a maximum metabolic rate at an optimum temperature, where metabolic rates are fastest:

$$T_{opt} = \frac{E_h T_h}{E_h + kT_h \ln\left(\frac{E_h}{E_a} - 1\right)} \quad (6)$$

The parameters $b(T_c)$, E_a, E_h, T_h and T_{opt} represent traits that together characterize the metabolic thermal response. We consider the parameters of this model to be traits that we expect to differ between isolates from the warmed and ambient mesocosms, reflecting local adaptation to the different temperature regimes. To test our hypotheses, we fitted the rate data to equation (5) using a non-linear mixed effects model via the 'nlme' package in R. Models included random effects by replicate on each of the parameters of the Sharpe–Schoolfield equation and 'selection environment' as a fixed two-level factor (for example, a 'warmed' or an 'ambient' isolate) on each parameter. Model selection proceeded in an identical manner to that described above. Results of model selection are detailed in Supplementary Tables 4 and 5.

Phenotypic plasticity in cell size. Cell size can exhibit substantial phenotypic plasticity (and does here) and vary as a function of temperature[35]. We therefore quantified the magnitude of phenotypic plasticity from the slope of the linear reaction norm of cell size with respect to temperature. To assess whether plasticity on cell size (slope) and/or cell size *per se* (intercept) differed between warmed versus ambient isolates, we fitted the cell size data to a linear mixed effects model, including random slopes and intercepts by replicates and 'assay temperature' (continuous covariate from 16 to 42 °C) and 'selection environment' (two-level factor, 'warmed' or 'ambient') as potentially interacting fixed effects. Model selection proceeded in an identical manner to that described above for the non-linear thermal reaction norms.

Determining competitive fitness. Competitive fitness was determined among all possible pairwise combinations of the warmed versus ambient isolates at both a high and a low temperature, yielding 160 combinations. Based on the outcome of the growth thermal responses, 16 and 34 °C were chosen to run the competition assays, as 34 °C was close to the optimum temperature for the warmed isolates and beyond the optima for the ambient isolates, and 16 °C was the average daytime temperature of the ambient mesocosms at the time of sampling. Assays were carried out in 12 well plates with inserts that had a 0.4 µm membrane base inserted into the well (Thinsert), allowing for extracellular products and nutrients to pass between the compartments while preventing the cells from doing so, enabling effective enumeration of each isolate in co-culture. We had previously established from the thermal responses of population growth that cells would be within the exponential phase at both assay temperatures at five days after inoculation. Specific growth rate, μ (d^{-1}), was calculated from cell counts at the beginning, and the end of the experiment, as $\mu = \frac{\ln(N_1 / N_0)}{\Delta T}$. where N_1 is cell density after five days, N_0 is the initial cell density, and ΔT is the time passed between measurements in days. Cell counts were made using flow cytometry. Competitive fitness of the warmed isolates was then calculated as the difference in specific growth rate between a warmed isolate, μ_i. and an ambient isolate, μ_j : $\Delta\mu_{ij} = \mu_i - \mu_j$.

As each warmed isolate was competed against all ambient isolates at two assay temperatures, these data have an inherent correlation structure in which fitness

coefficients for a given isolate will be auto-correlated. We therefore analysed these data using a linear mixed effects model. We accounted for non-independence in fitness coefficients derived from a given focal isolate by including its identity as a random effect on the intercept of the model. 'Assay temperature' (16 and 34 °C) was then modelled as a fixed factor and we used a post-hoc Tukey test ('glht' in the 'multcomp' package in R) to determine whether competitive fitness of the warmed isolates was significantly different from zero at 16 and 34 °C, and whether coefficients at 16 °C differed significantly from those at 34 °C.

Linking competitive fitness and metabolism. We hypothesized that increased photosynthesis was an important determinant of adaptation to warming. To test this hypothesis, we assessed whether rates of NP differed between warmed versus ambient isolates at the two assay temperatures in which the competition trials were carried out (for example, 16 and 34 °C). We analysed these data using a linear mixed effects model to account for the hierarchical and unbalanced nature of the data. Replicate-level variation was treated as a random effect on the intercept of the model and assay temperature (16 and 34 °C), and selection environment ('warmed' or 'ambient') were modelled as potentially interacting fixed factors. Model selection was as described above.

Finally, we assessed whether evolved differences in rates of NP between warmed and ambient isolates were a driver of competitive fitness. To do so, we determined whether pairwise differences in NP between warmed and ambient isolates, $\Delta NP_{ij} = NP_i - NP_j$, were a significant predictor of the competitive fitness of the warmed isolates, $\Delta\mu_{ij} = \mu_i - \mu_j$, where i and j denote the rates of NP and μ for warmed isolates i and ambient isolates j, respectively. As before, because any given isolate was competed against all others from the opposing treatment, these data have an inherent autocorrelation structure. We therefore analysed these data using a linear mixed effects model in which the competitive fitness was the dependent variable, ΔNP_{ij} was a continuous covariate and assay temperature (for example, 16 and 34 °C) was a fixed factor. We accounted for non-independence in the data by including isolate identity as a random effect on the intercept of the model. Model selection was as described above.

Data availability. 18S sequences are stored in Genbank (see Supplementary Table 1 for accession numbers). Data used for graphs and analysis are available in Supplementary Data 1.

Received 23 June 2016; accepted 19 January 2017; published 20 March 2017

References

1. Falkowski, P. G. Biogeochemical controls and feedbacks on ocean primary production. *Science* **281,** 200–206 (1998).
2. Raven, J. A. & Falkowski, P. G. Oceanic sinks for atmospheric CO_2. *Plant Cell Environ.* **22,** 741–755 (1999).
3. Field, C. B. Primary production of the biosphere: integrating terrestrial and oceanic components. *Science* **281,** 237–240 (1998).
4. Falkowski, P. G. The role of phytoplankton photosynthesis in global biogeochemical cycles. *Photosynth. Res.* **39,** 235–258 (1994).
5. Bopp, L. *et al.* Potential impact of climate change on marine export production. *Glob. Biogeochem. Cycles* **15,** 81–99 (2001).
6. López-Urrutia, Á., Martin, E. S., Harris, R. P. & Irigoien, X. Scaling the metabolic balance of the oceans. *Proc. Natl Acad. Sci. USA* **103,** 8739–8744 (2006).
7. Laufkötter, C. *et al.* Drivers and uncertainties of future global marine primary production in marine ecosystem models. *Biogeosciences* **12,** 6955–6984 (2015).
8. Regaudie-de-Gioux, A. & Duarte, C. M. Compensation irradiance for planktonic community metabolism in the ocean. *Glob. Biogeochem. Cycles* **24,** GB4013 (2010).
9. Schluter, L. *et al.* Adaptation of a globally important coccolithophore to ocean warming and acidification. *Nat. Clim. Change* **4,** 1024–1030 (2014).
10. Padfield, D., Yvon-Durocher, G., Buckling, A., Jennings, S. & Yvon-Durocher, G. Rapid evolution of metabolic traits explains thermal adaptation in phytoplankton. *Ecol. Lett.* **19,** 133–142 (2015).
11. Listmann, L., LeRoch, M., Schluter, L., Thomas, M. K. & Reusch, T. B. H. Swift thermal reaction norm evolution in a key marine phytoplankton species. *Evol. Appl.* **9,** 1156–1164 (2016).
12. Raven, J. A. & Geider, R. J. Temperature and algal growth. *New Phytol.* **110,** 441–461 (1988).
13. Lawrence, D., Bell, T. & Barraclough, T. G. The effect of immigration on the adaptation of microbial communities to warming. *Am. Nat.* **187,** 236–248 (2016).
14. Lawrence, D. *et al.* Species interactions alter evolutionary responses to a novel environment. *PLoS Biol.* **10,** e1001330 (2012).
15. Collins, S. Competition limits adaptation and productivity in a photosynthetic alga at elevated CO_2. *Proc. R. Soc. B* **278,** 247–255 (2010).
16. Yvon-Durocher, G., Jones, J. I., Trimmer, M., Woodward, G. & Montoya, J. M. Warming alters the metabolic balance of ecosystems. *Phil. Trans. R. Soc. B* **365,** 2117–2126 (2010).
17. Yvon-Durocher, G. *et al.* Five years of experimental warming increases the biodiversity and productivity of phytoplankton. *PLoS Biol.* **13,** e1002324 (2015).
18. Geider, R. J., MacIntyre, H. L. & Kana, T. M. Dynamic model of phytoplankton growth and acclimation: responses of the balanced growth rate and the chlorophyll *a*:carbon ratio to light, nutrient-limitation and temperature. *Mar. Ecol. Prog. Ser.* **144,** 187–200 (1997).
19. Badger, M. R., von Caemmerer, S., Ruuska, S. & Nakano, H. Electron flow to oxygen in higher plants and algae: rates and control of direct photoreduction (Mehler reaction) and rubisco oxygenase. *Phil. Trans. R. Soc. B* **355,** 1433–1446 (2000).
20. Houille-Vernes, L. & Rappaport, F. Plastid terminal oxidase 2 (PTOX2) is the major oxidase involved in chlororespiration in *Chlamydomonas*. *Proc. Natl Acad. Sci. USA* **108,** 20820–20825 (2011).
21. Erickson, E., Wakao, S. & Niyogi, K. K. Light stress and photoprotection in *Chlamydomonas reinhardtii*. *Plant J.* **82,** 449–465 (2015).
22. Atkin, O. K. *et al.* Global variability in leaf respiration in relation to climate, plant functional types and leaf traits. *New Phytol.* **206,** 614–636 (2015).
23. Yvon-Durocher, G., Dossena, M., Trimmer, M., Woodward, G. & Allen, A. P. Temperature and the biogeography of algal stoichiometry. *Glob. Ecol. Biogeogr.* **24,** 562–570 (2015).
24. Toseland, A. *et al.* The impact of temperature on marine phytoplankton resource allocation and metabolism. *Nat. Clim. Change* **3,** 979–984 (2013).
25. Berman-Frank, I. & Dubinsky, Z. Balanced growth in aquatic plants: myth or reality? Phytoplankton use the imbalance between carbon assimilation and biomass production to their strategic advantage. *BioScience* **49,** 29–37 (1999).
26. Yvon-Durocher, G., Montoya, J. M., Trimmer, M. & Woodward, G. Warming alters the size spectrum and shifts the distribution of biomass in freshwater ecosystems. *Glob. Change Biol.* **17,** 1681–1694 (2011).
27. IPCC *Climate Change 2014: Synthesis Report* (eds Pachauri, R. K. & Meyer, L. A.) (Cambridge Univ. Press, 2014).
28. Nakada, T., Shinkawa, H., Ito, T. & Tomita, M. Recharacterization of *Chlamydomonas reinhardtii* and its relatives with new isolates from Japan. *J. Plant Res.* **123,** 67–78 (2009).
29. Rambaut, A. FigTree version 1.4.2. (2014); http://tree.bio.ed.ac.uk/software/figtree/
30. Buchanan, R. L., Whiting, R. C. & Damert, W. C. When is simple good enough: a comparison of the Gompertz, Baranyi, and three-phase linear models for fitting bacterial growth curves. *Food Microbiol.* **14,** 313–326 (1997).
31. Elzhov, T. V., Mullen, K. M., Spiess, A. N. & Bolker, B. minpack.lm: R interface to the Levenberg-Marquardt nonlinear least-squares algorithm found in MINPACK, plus support for bounds. R package version 1.2-1 (2013); https://cran.r-project.org/web/packages/minpack.lm/index.html
32. Edwards, K. F., Thomas, M. K., Klausmeier, C. A. & Litchman, E. Phytoplankton growth and the interaction of light and temperature: a synthesis at the species and community level. *Limnol. Oceanogr.* **61,** 1232–1244 (2016).
33. Eilers, P. H. C. & Peeters, J. C. H. A model for the relationship between light intensity and the rate of photosynthesis in phytoplankton. *Ecol. Model.* **42,** 199–215 (1988).
34. Suggett, D. J., Moore, C. M., Hickman, A. E. & Geider, R. J. Interpretation of fast repetition rate (FRR) fluorescence: signatures of phytoplankton community structure versus physiological state. *Mar. Ecol. Prog. Ser.* **376,** 1–19 (2009).
35. Atkinson, D., Ciotti, B. J. & Montagnes, D. J. S. Protists decrease in size linearly with temperature: ca. 2.5% $°C^{-1}$. *Proc. R. Soc. B* **270,** 2605–2611 (2003).

Acknowledgements

This study was supported by a grant from the Leverhulme Trust (RPG-2013-335) awarded to G.Y.-D, A.B. and N.S., and an NERC grant awarded to S.P. and G.Y.-D. (NE/M003205/1).

Author contributions

G.Y.-D. conceived the study. C.-E.S. and G.Y.-D. designed the experimental work, and P.L., C.-E.S., S.B. and E.B. conducted the experiment. C.-E.S. and G.Y.-D. analysed the data. M.T. maintains the experimental mesocosms. C.-E.S. and G.Y.-D. wrote the manuscript and all authors contributed to revisions.

Additional information

Supplementary information is available for this paper.

Reprints and permissions information is available at www.nature.com/reprints.

Correspondence and requests for materials should be addressed to G.Y.-D. or C.-E.S.

How to cite this article: Schaum, C.-E. *et al.* Adaptation of phytoplankton to a decade of experimental warming linked to increased photosynthesis. *Nat. Ecol. Evol.* **1,** 0094 (2017).

Competing interests

The authors declare no competing financial interests.